

Parabolic polygons and discrete affine geometry

MARCOS CRAIZER¹, THOMAS LEWINER¹ AND JEAN-MARIE MORVAN²

¹ Department of Mathematics — Pontifícia Universidade Católica — Rio de Janeiro — Brazil

² Université Claude Bernard — Lyon — France

{craizer, tomlew}@mat.puc--rio.br. jean--marie.morvan@sophia.inria.fr.

Abstract. Geometry processing applications estimate the local geometry of objects using information localized at points. They usually consider information about the normal as a side product of the points coordinates. This work proposes parabolic polygons as a model for discrete curves, which intrinsically combines points and normals. This model is naturally affine invariant, which makes it particularly adapted to computer vision applications. This work introduces estimators for affine length and curvature on this discrete model and presents, as a proof-of-concept, an affine invariant curve reconstruction.

Keywords: *Affine Differential Geometry. Affine Curvature. Affine Length. Curve Reconstruction.*

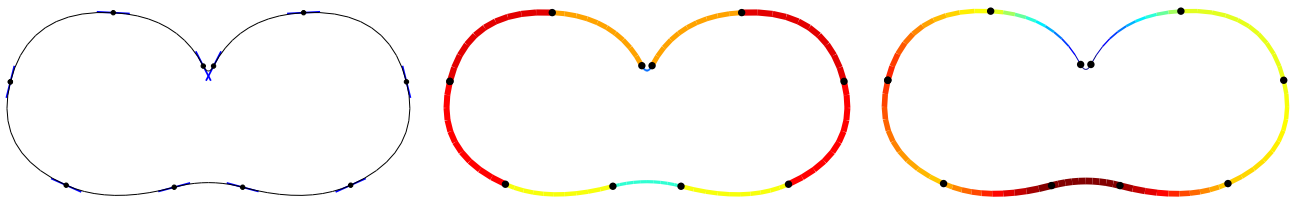


Figure 1: Example of a parabolic polygon with 10 arcs (left), our estimation of their affine length (middle) and affine curvature (right).

1 Introduction

Geometric objects are represented by discrete structures for computer applications. These structures usually rely on pointwise information combined with adjacency relations. Most geometry processing applications require the normal of the object at each point: either for rendering [10], evolution [4], or numerical stability of reconstruction [1]. Modern Geometry acquisition processes for curves or surfaces usually provide measures of the normals together with the point measures. These normals can also be robustly estimated only from the point coordinates [11, 7].

However, the normal or tangent information is usually considered separately from the point coordinate, and the definition of the geometrical object depends rather on the point coordinates. Although modelling already makes intensive use of this information, in particular with Bézier curves, only recent developments in reconstruction problems proposed to incorporate these tangents as part of the point set definition [1].

In this work, we propose a discrete curve representa-

tion based on points and tangents: the parabolic polygons, introduced in section 2 *Parabolic polygons*. This model is naturally invariant with respect to affine transformations of the plane. As opposed to implicit affine representations [12], our representation uses only local information. This makes it particularly adapted to computer vision applications, since two contours of the same planar object obtained from different perspectives are approximately affine equivalent.

In section 4 *Affine estimates*, we propose geometric estimators that are affine invariant, which makes the model effective for applications. The theoretical validity of our estimators is verified on representative cases, as can be seen in section 5 *Convergence issues*. In section 6 *Experimental results*, the practical validity of the estimators is verified on samples of analytic curves.

The only works we are aware about affine curvature estimators are due to Calabi, Olver, Tannenbaum et al. [8, 9] and Boutin [2]. They estimate affine curvature from five consecutive samples, by interpolating these points by a conic. The affine curvature at the central point is then estimated by the affine curvature of that conic. They further prove that this estimator derives from discrete affine volume forms, which are the only affine invariant forms for points.

With the conciseness of parabolic polygons, we estimate the affine curvature from just three consecutive points, which is well suited for applications such as reconstruction, interpolation and blending.

For the application in curve reconstruction of section 7 *Affine curve reconstruction*, we changed the distance computation in [5] by our affine estimates. This leads to an affine invariant curve reconstruction, which works well on synthetic examples. Moreover, we observed that the introduction of the curvature in the algorithm improves the stability of the reconstruction, thus pledging for the validity of our affine curvature estimator.

2 Parabolic polygons

When we consider just the position of the sample points of a curve as the data, it is natural to connect them by line segments, thus forming a Euclidean polygon. In our model, each point carries more information: Besides its position, we know also its tangent line. Then it is natural to connect a pair of points by an arc of parabola that passes through and is tangent to the tangent line at each point. The "polygon" thus formed will be called a *parabolic polygon* (see Figure 1).

Consider a curve γ in the plane. If l_i and l_{i+1} are the tangent lines at \mathbf{x}_i and \mathbf{x}_{i+1} of a convex arc of γ , then l_i is not parallel to l_{i+1} . We shall assume that we are given a finite sequence of points $\{\mathbf{x}_1, \dots, \mathbf{x}_n\}$ and lines $\{l_1, \dots, l_n\}$ passing through the points such that l_i is not parallel to l_{i+1} , for any $1 \leq i \leq n$.

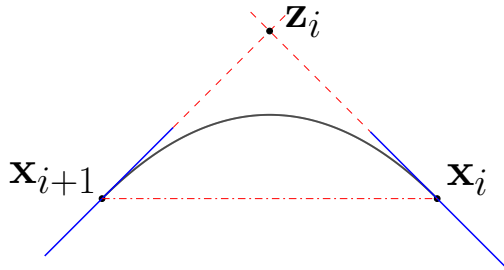


Figure 2: Support triangle.

Support point and support triangle. Denote by z_i the point of intersection of l_i and l_{i+1} . This point is called the *support point* and the triangle $(\mathbf{x}_i, z_i, \mathbf{x}_{i+1})$ is called the *support triangle*. As pointed out in [8] the cubic root of the area A_i of the support triangle is a good measure of the distance between (\mathbf{x}_i, l_i) and $(\mathbf{x}_{i+1}, l_{i+1})$.

Parabolic arcs. For each pair of consecutive indexes $(i, i + 1)$, denote by P_i the unique parabolic arc passing through \mathbf{x}_i and \mathbf{x}_{i+1} with tangent lines l_i and l_{i+1} at these points. The parabolic polygon obtained by the concatenation of P_i , $1 \leq i \leq n - 1$, will be denoted by P .

3 Affine length and curvature

This section quickly recalls the definitions of the relevant affine quantities. The reader will find a detailed presentation of affine geometry in Buchin's book [3].

Affine length. Consider a smooth curve γ in the plane. Take a convex arc of γ and parameterize it by $\mathbf{x}(t)$, $t_0 \leq t \leq t_1$, with $\mathbf{x}'(t) \wedge \mathbf{x}''(t) > 0$. The number

$$s(t) = \int_{t_0}^t \mathbf{x}'(t) \wedge \mathbf{x}''(t)^{\frac{1}{3}} dt$$

is called the affine parameter of the arc. Observe that s can be characterized by the equation

$$\mathbf{x}'(s) \wedge \mathbf{x}''(s) = 1. \quad (1)$$

The affine length L of the arc is defined by $L = s(t_1) - s(t_0)$.

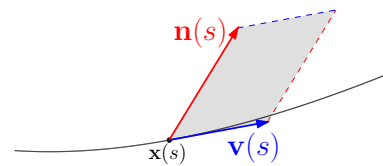


Figure 3: Affine tangent $\mathbf{v}(s)$ and normal $\mathbf{n}(s)$. The area of the parallelogram is equal to 1.

Affine tangent and normal. The first derivative $\mathbf{x}'(s)$ is called the *affine tangent* and is tangent to the curve. It will be denoted by $\mathbf{v}(s)$. The second derivative $\mathbf{x}''(s)$ is called the *affine normal* and will be denoted by $\mathbf{n}(s)$. Observe that the affine normal is not necessarily perpendicular to the curve in the Euclidean sense.

Affine curvature. Differentiating equation (1), we obtain that $\mathbf{x}'(s)$ and $\mathbf{x}'''(s)$ are co-linear. The *affine curvature* $\mu(s)$ is defined by the equation

$$\mathbf{x}'''(s) = -\mu(s)\mathbf{x}'(s).$$

One can also define the affine curvature by $\mu(s) = \mathbf{x}''(s) \wedge \mathbf{x}'''(s)$.

Affine behaviour of inflections. In section 7 *Affine curve reconstruction*, it will be important for us to understand the behaviour of the affine quantities near a higher order tangent. This behaviour can be well observed in the following example:

Consider the curve $\mathbf{x}(t) = (t, t^n)$, $n \geq 3$, $0 \leq t \leq 1$, which has a higher order tangent at $t = 0$ (see Figure 4). Easy calculations show that, for $c > 0$,

$$\mathbf{x}(s) = \left(cs^{\frac{3}{n+1}}, c^n s^{\frac{3n}{n+1}} \right)$$

is an affine parameterization of the curve. Thus we have that the affine tangent

$$\mathbf{v}(s) = \left(\frac{3c}{n+1} s^{\frac{2-n}{n+1}}, \frac{3nc^n}{n+1} s^{\frac{2n-1}{n+1}} \right)$$

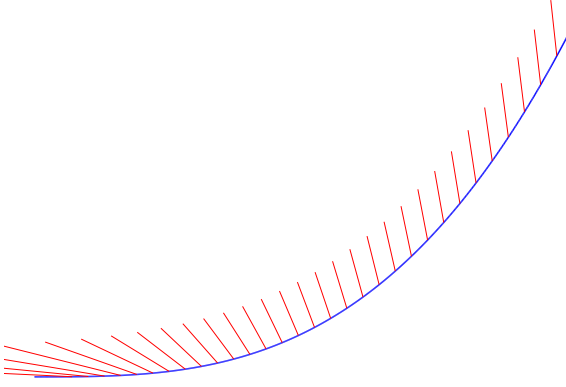


Figure 4: The affine normal of a cubic near its inflection point.

converges to an infinite length vector in the positive x -direction, when $s \rightarrow 0$. The affine normal

$$\mathbf{n}(s) = \left(\frac{3c(2-n)}{(n+1)^2} s^{\frac{1-2n}{n+1}}, \frac{3nc^n(2n-1)}{(n+1)^2} s^{\frac{n-2}{n+1}} \right).$$

also converges to an infinite length vector in the x -direction, but in the negative sense (see Figure 4). The affine curvature is given by

$$\mu(s) = \frac{(n-2)(2n-1)}{(n+1)^2} s^{-2}.$$

4 Affine estimates

We will now propose an affine length estimator and an affine curvature estimator for a parabolic polygon.

Affine length. Denote by L_i the affine length of the parabolic arc P_i and by \mathbf{n}_i its affine normal. In [8], it is proved that $L_i = 2A_i^{\frac{1}{3}}$, where A_i is the area of the support triangle. The affine length of a parabolic polygon P is the sum of the affine lengths L_i of the parabolic arcs P_i .

Affine normal. The expression for \mathbf{n}_i is given in the following lemma:

Lemma 1 Denote by $\mathbf{v}_{i,1}$ and $\mathbf{v}_{i,2}$ the affine tangents of the parabola P_i at \mathbf{x}_i and \mathbf{x}_{i+1} , respectively. If the support triangle $(\mathbf{x}_i, \mathbf{z}_i, \mathbf{x}_{i+1})$ is positively oriented, then

$$\begin{aligned} \mathbf{v}_{i,1} &= -\frac{2}{L_i} (\mathbf{x}_i - \mathbf{z}_i) \\ \mathbf{v}_{i,2} &= \frac{2}{L_i} (\mathbf{x}_{i+1} - \mathbf{z}_i) \end{aligned}$$

If the support triangle is negatively oriented, the signs must be interchanged. In any case

$$\mathbf{n}_i = \frac{2}{L_i^2} (\mathbf{x}_i + \mathbf{x}_{i+1} - 2\mathbf{z}_i).$$

Proof: Just observe that the parabola

$$\gamma(s) = \mathbf{x}_i + s\mathbf{v}_{i,1} + \frac{s^2}{2}\mathbf{n}_i$$

is parameterized by arc length and passes through \mathbf{x}_i and \mathbf{x}_{i+1} with tangent lines l_i and l_{i+1} , respectively. ■

Affine curvature. Consider a convex arc C in E^2 . Then

$$\int_C \mu ds = \int_C \mathbf{n}'(s) \wedge \mathbf{n}(s) ds$$

can be approximated by

$$\sum \left(\frac{\mathbf{n}(s+\Delta s) - \mathbf{n}(s)}{\Delta s} \wedge \mathbf{n}(s) \right) \Delta s = \sum \mathbf{n}(s+\Delta s) \wedge \mathbf{n}(s).$$

We propose as a definition of the integral of the affine curvature along a parabolic polygon the sum

$$\mu(P) = \sum_{i=2}^{n-1} \mathbf{n}_{i-1} \wedge \mathbf{n}_i.$$

5 Convergence issues

Consider a convex arc C in E^2 . Let (\mathbf{x}_i, l_i) , $1 \leq i \leq n$ be a sampling of the curve, where l_i is the line tangent to C at \mathbf{x}_i . Assume that the sampling points are equally spaced, i.e., that the affine length between sample points along the curve is equal to L/n , where L is the affine length of the curve. We say that the affine length estimator is *convergent* if $\sum_{i=1}^{n-1} L_i$ converge to the affine length L of the curve, when $n \rightarrow \infty$. And that the affine curvature estimator is convergent if $\mu(P)$ converges to $\int_C \mu(s) ds$, when $n \rightarrow \infty$.

In [8, p.14], it is shown the convergence of the affine lengths estimator. In the rest of the section, we shall consider the particular case of constant affine curvature curves. For these curves, we compute explicitly the estimators to show the convergence of the affine length and of the affine curvature. The experiments of section 6 *Experimental results* also indicate that our affine curvature estimator is convergent.

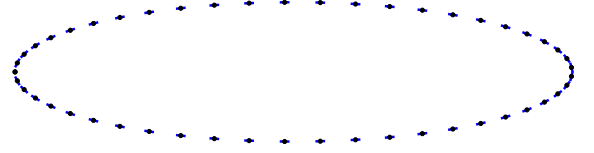
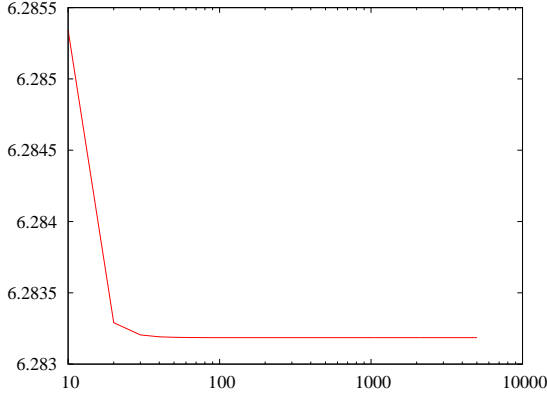
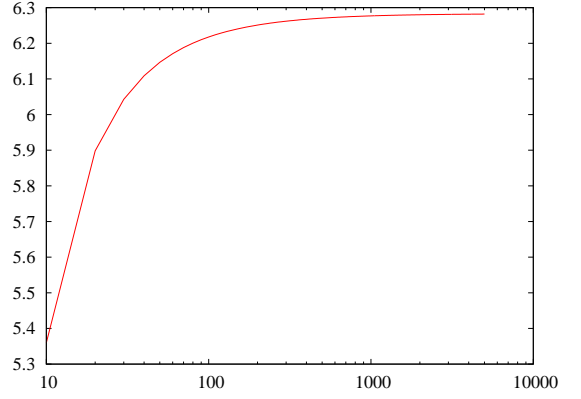


Figure 5: Fifty affine equally spaced samples of an ellipse.

Positive curvature. In this example, we consider the case of a curve with constant positive affine curvature (see Figure 5). By making an affine transformation of the plane, we can assume that this curve is a circle. Consider points



6(a): Estimated affine length vs number of samples.



6(b): Estimated integral of the affine curvature vs number of samples.

Figure 6: Convergence of the estimators for the positive curvature case with $R = 1$.

(x_i, y_i) , $1 \leq i \leq n$, in a circle of radius R at an affine distance $s = L/n$, where $L = 2\pi R^{\frac{2}{3}}$ is the affine length of the circle. The affine curvature of this circle is $\mu = R^{-\frac{4}{3}}$. The central angle determined by two consecutive points is $2\alpha = \frac{2\pi}{n}$.

Simple calculations show that the affine length of the arc of parabola P_i is given by

$$L_i = \frac{2R^{\frac{2}{3}} \sin \alpha}{\cos^{\frac{1}{3}} \alpha}$$

and that the affine normal is orthogonal to the chord connecting (x_i, y_i) and (x_{i+1}, y_{i+1}) , with norm

$$\|\mathbf{n}_i\| = R^{-\frac{1}{3}} \cos^{-\frac{1}{3}} \alpha.$$

Thus the estimated affine curvature is given by

$$\mathbf{n}_i \wedge \mathbf{n}_{i+1} = R^{-\frac{2}{3}} \cos^{-\frac{2}{3}}(\alpha) \sin(2\alpha).$$

The estimated affine length of the circle is then

$$\sum_{i=1}^{n-1} L_i = 2R^{\frac{2}{3}} (n-1) \frac{\sin\left(\frac{\pi}{n}\right)}{\cos^{\frac{1}{3}}\left(\frac{\pi}{n}\right)}$$

which converges to the affine length of the circle when $n \rightarrow \infty$ (see Figure 6(a)). And the estimated affine length

$$\mu(P) = (n-2) R^{-\frac{2}{3}} \cos^{-\frac{2}{3}}\left(\frac{\pi}{n}\right) \sin\left(\frac{2\pi}{n}\right)$$

converges to $2\pi R^{-\frac{2}{3}} = L\mu$, when $n \rightarrow \infty$ (see Figure 6(b)).

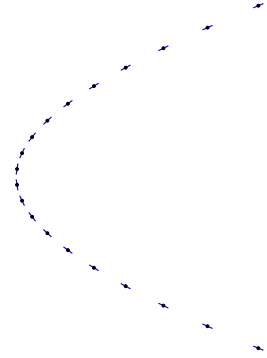
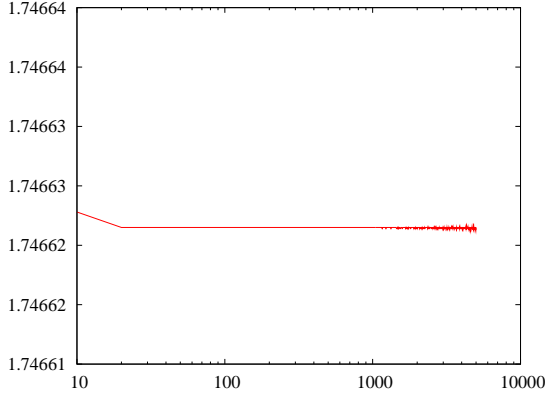


Figure 7: Twenty affine equally spaced samples of a hyperbola.

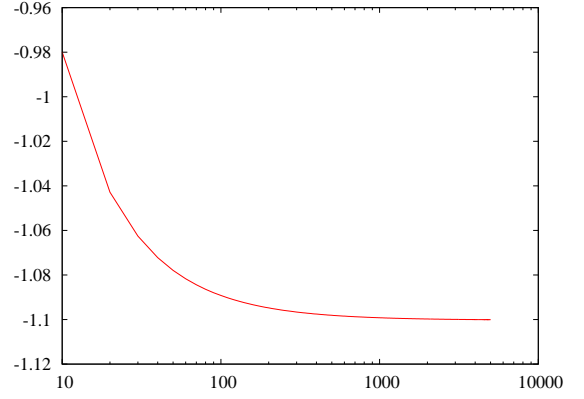
Negative curvature. In this example, we consider the case of a curve with constant negative affine curvature (see Figure 7). By making an affine transformation of the plane, we can assume that this curve is a hyperbola $xy = c$, for some $c > 0$. Consider points (x_i, y_i) , $1 \leq i \leq n$, in the hyperbola at an affine distance $s = L/n$, where $L = (2c)^{\frac{1}{3}} \ln(x_n/x_1)$ is the affine length of the arc of hyperbola between (x_1, y_1) and (x_n, y_n) . The affine curvature of this hyperbola is $\mu = -(2c)^{-\frac{2}{3}}$.

Denote by $r = \frac{x_{i+1}}{x_i} = \frac{y_i}{y_{i+1}}$. From the fact that the affine lengths between (x_i, y_i) and (x_{i+1}, y_{i+1}) along the hyperbola is $(2c)^{\frac{1}{3}} \ln(r)$, one conclude that r does not depend on i . Straightforward calculations shows that the area of the support triangle defined by (x_i, y_i) and (x_{i+1}, y_{i+1}) is given by $c \frac{(r-1)^3}{2r(r+1)}$ and so the affine length of P_i is given by

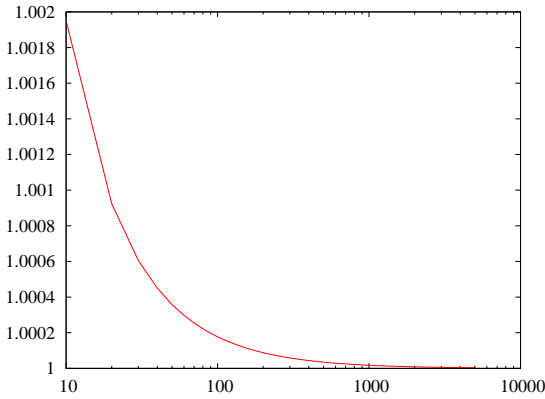
$$L_i = \left(\frac{4c}{(r+1)r} \right)^{\frac{1}{3}} (r-1).$$



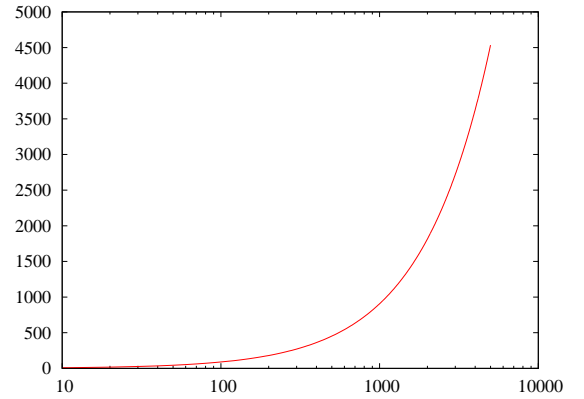
8(a): Estimated affine length vs number of samples.



8(b): Estimated integral of the affine curvature vs number of samples.

Figure 8: Convergence of the estimators for the negative curvature case, with $c = 1$.

9(a): Estimated affine length vs number of samples.



9(b): Estimated integral of the affine curvature vs number of samples.

Figure 9: Convergence of the estimators for a cubic with $y = x^3$, $x \in [0, \frac{2}{3}\sqrt[4]{2}]$.

Also, the affine normal to P_i is given by

$$\mathbf{n}_i = \left(\frac{r^2}{2(r+1)c^2} \right)^{\frac{1}{3}} (x_i, y_{i+1}),$$

and so

$$\mathbf{n}_{i-1} \wedge \mathbf{n}_i = \left(\frac{r+1}{4cr^2} \right)^{\frac{1}{3}} (1-r).$$

We conclude that

$$\sum_{i=1}^{n-1} L_i = (n-1) \left(\frac{4c}{(r+1)r} \right)^{\frac{1}{3}} (r-1)$$

converges to L (see Figure 8(a)). And that the estimated affine curvature of the arc

$$\sum_{i=2}^{n-1} \mathbf{n}_{i-1} \wedge \mathbf{n}_i = (n-2) \left(\frac{r+1}{4cr^2} \right)^{\frac{1}{3}} (1-r)$$

converges to $(2c)^{-\frac{1}{3}} \ln(x_n/x_1) = L\mu$ (see Figure 8(b)).

6 Experimental results

We have tested the above estimates on samples analytic curves. In section 5 *Convergence issues*, the cases of constant affine curvature were tested. In this section, we test the cubic $y = x^3$, $0 \leq x \leq \frac{2}{3}\sqrt[4]{2}$.

In Figure 9, we can see the convergence of the affine length and of the affine curvature when the number of samples grows. It is interesting to observe that the affine length is a non-increasing function of the number of samples, as pointed out in [8]. Another important property of our estimators is their affine invariance, which can be observed in Figure 10.

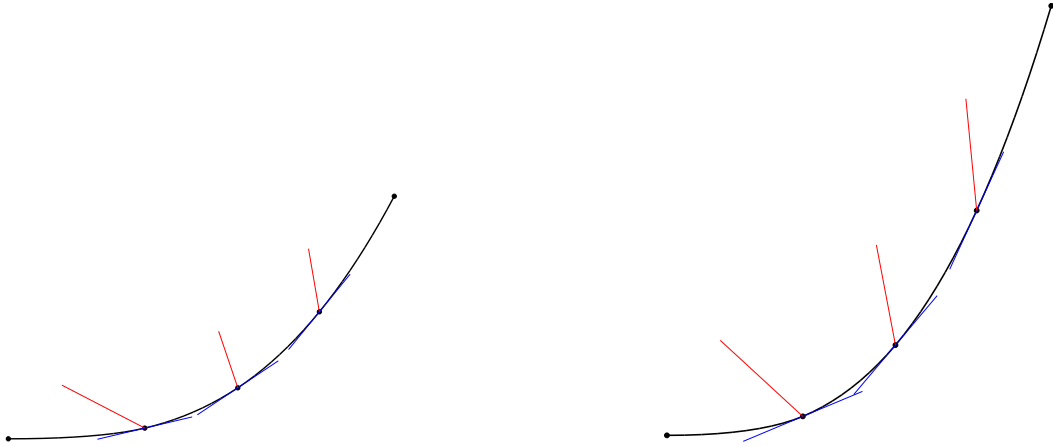
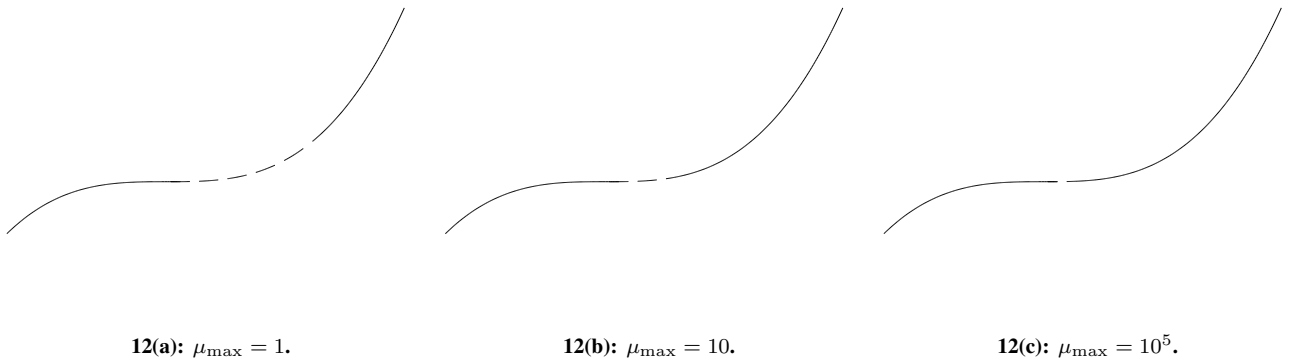


Figure 10: Invariance with respect to the affine transform $x \mapsto \frac{3}{4}x, y \mapsto \frac{4}{3}y$: our estimators gave exactly the same values for both cases: lengths 0.254381, 0.250007, 0.250001 and 0.250000, curvatures 11.0122, 1.40326, and 0.583464.



12(a): $\mu_{\max} = 1$.

12(b): $\mu_{\max} = 10$.

12(c): $\mu_{\max} = 10^5$.

Figure 12: Reconstruction close to an inflection point.

7 Affine curve reconstruction

In this section, we consider the following problem to validate our parabolic polygon model and the related affine estimators: Given a finite sequence of points $\{\mathbf{x}_1, \dots, \mathbf{x}_n\}$ and tangent lines $\{l_1, \dots, l_n\}$ passing through the points, we look for a parabolic polygon that is in some sense close to the original curve. We propose an algorithm that will combine the affine invariance of our model with the ability

to use the tangent as intrinsic information. The estimator of affine curvature proposed above is used in the algorithm in a way similar to [6, 5].

The algorithm works as follows: In the first step of the algorithm one look at the pair $(\mathbf{x}_i, l_i), (\mathbf{x}_j, l_j)$ which have the smallest affine distance. Then we proceed in a greedy fashion to find the next pair (\mathbf{x}_k, l_k) which is at a minimum affine distance of one of the ends of the reconstructed curve. We validate he optimal pair (\mathbf{x}_k, l_k) as follows:

1. If the affine curvature of arc $(\mathbf{x}_i, l_i), (\mathbf{x}_j, l_j), (\mathbf{x}_k, l_k)$ is smaller than threshold μ_{\max} , the point is accepted.
2. If the affine curvature is bigger than μ_{\max} , two things may occur:
 - (a) either the pair (\mathbf{x}_k, l_k) induces an undesirable deviation, and the point is rejected,
 - (b) or we are close to a higher order tangent, such as an inflection point, and the point is accepted.

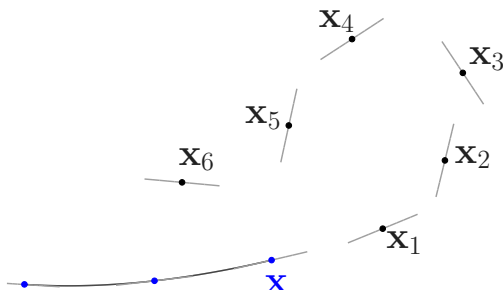


Figure 11: Point \mathbf{x}_5 is at the smallest affine distance of \mathbf{x} , but it is rejected because it would induce a big affine curvature.

As we have seen in section 3 *Affine length and curvature*, cases 2(a) and 2(b) can be characterized by the product $\mathbf{n}_{ij} \wedge \mathbf{n}_{jk}$

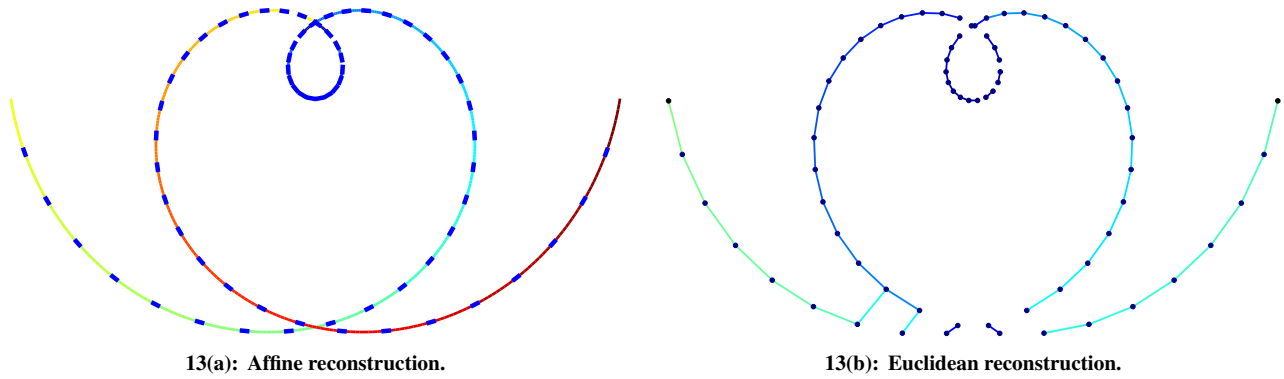


Figure 13: Our intrinsic use of tangents improves the reconstruction.

between the affine normals of each parabolic arc: $\mathbf{n}_{ij} \wedge \mathbf{n}_{jk}$ is small in case 2(a) and big in case 2(b) (see Figure 11).

If the point is rejected, we continue our greedy selection for completing the curve with another pair (\mathbf{x}_k, l_k) . If the point is close to a higher order tangent, the algorithm completes the curve with (\mathbf{x}_k, l_k) , but stops on that end (Figure 12), as explained below.

In our algorithm, we reconstruct only the convex arcs of the curve, since passing through inflection points is very delicate. The parameter μ_{\max} controls how much we can get close to an inflection point. The bigger we take μ_{\max} , closer we can get to the inflection point (see Figure 12). But we cannot take μ_{\max} very big because in this case we would accept undesirable deviations (see Figure 11).

We compared our parabolic polygon model with affine estimates with the classical Euclidean polygon model. The algorithm used for the Euclidean reconstruction is based on [5], using the curvature as described in the affine case but not the information of the tangents. In Figure 13, we can observe how the intrinsic use of the tangent information of our model improves the result. In Figure 14, we can check the affine invariance of the reconstruction algorithm, and the non-affine invariance of its Euclidean version. Moreover, we can see the importance of the tangent information at cusps.

8 Conclusion

In this work we propose the parabolic polygon as a model for discrete curves that combine intrinsically the position and the tangent line of each sample. This model has the property of being affine invariant, which makes it particularly interesting for computer vision. Based on this model, we propose an affine length estimator and an affine curvature estimator. The validity of these estimators was checked on a curve reconstruction application.

As future work, we intend to consider the corresponding problems in 3D. One of the important questions in this context is how to estimate the affine area and curvatures

of a surface given by sample points and normals.

References

- [1] N. Amenta and Y. J. Kil. Defining point-set surfaces. *Transaction on Graphics*, 23(3):264–270, 2004.
- [2] M. Boutin. Numerically invariant signature curves. *International Journal of Computer Vision*, 40(3):235–248, 2000.
- [3] S. Buchin. *Affine Differential Geometry*. Academic Press, 1982.
- [4] L. D. Cohen. On active contour models and balloons. *Computer Vision and Image Understanding*, 2(53):211–218, 1991.
- [5] L. H. Figueiredo and J. M. Gomes. Computational morphology of curves. *Visual Computer*, 11:105–112, 1994.
- [6] H. Hoppe, T. de Rose, T. Duchamp, J. M. Donald and W. Stuetzle. Surface reconstruction from unorganized points. In *Siggraph*, pages 71–78, 1992.
- [7] N. J. Mitra and A. T. Nguyen. Estimating surface normals in noisy point cloud data. In *Symposium on Computational Geometry*, pages 322 – 328, 2003.
- [8] E. Calabi, P. J. Olver and A. Tannenbaum. Affine geometry, curve flows, and invariant numerical approximations. *Advances in Mathematics*, 124:154–196, 1997.
- [9] E. Calabi, P. J. Olver, C. Shakiban, A. Tannenbaum and S. Hacker. Differential and numerically invariant signature curves applied to object recognition. *International Journal of Computer Vision*, 26(2):107–135, 1998.
- [10] B. T. Phong. Illumination for computer generated pictures. *Communication of the ACM*, 18(6):311–317, 1975.
- [11] C.-K. Tang, M.-S. Lee and G. Medioni. Tensor Voting. In *Recent Advances in Perceptual Organization*. Kluwer, 2006.
- [12] W. A. Wolovich and M. Unel. The Determination of Implicit Polynomial Canonical Curves. *Transactions on Pattern Analysis and Machine Intelligence*, 20(10):1080–1090, 1998.

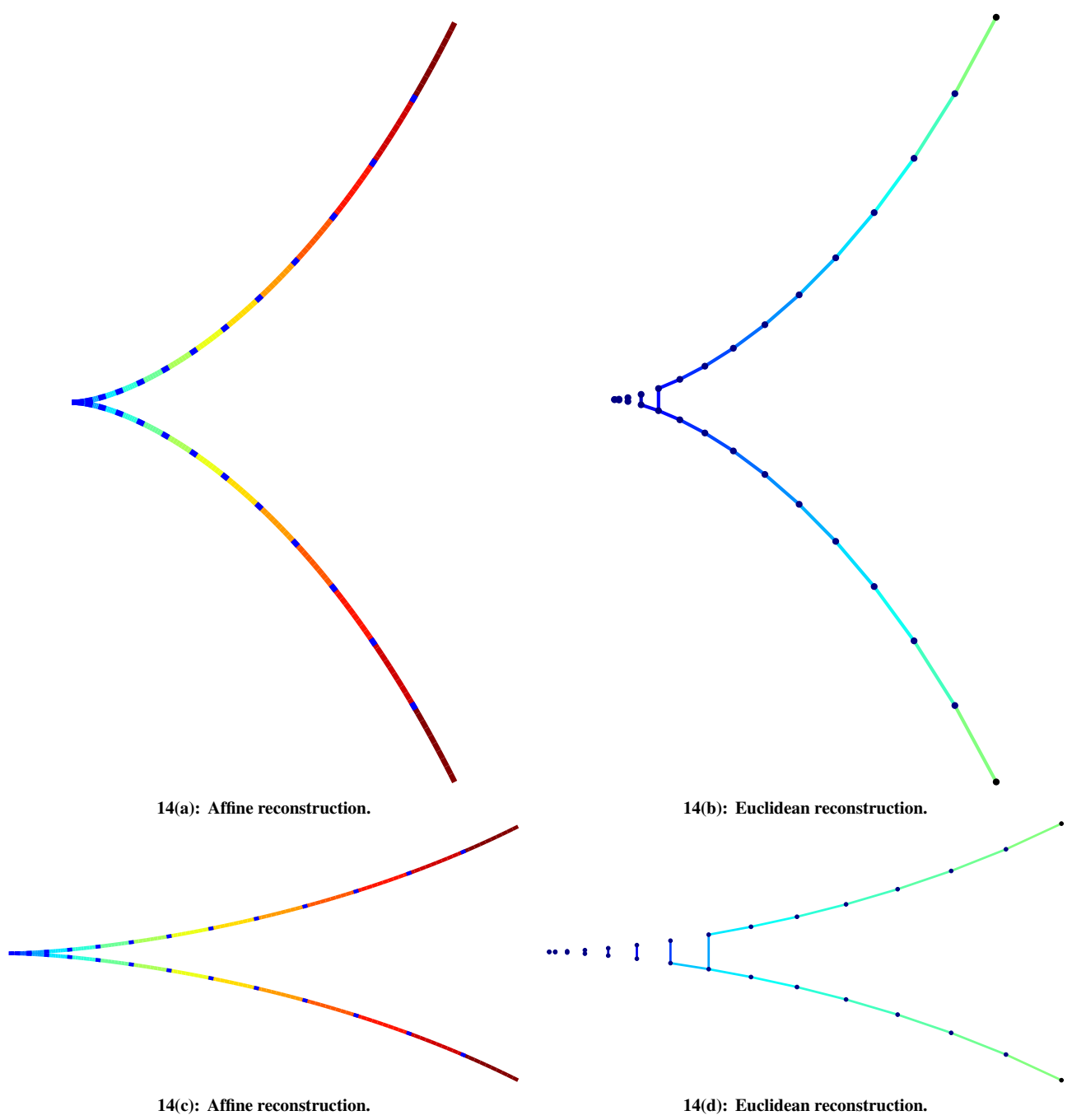


Figure 14: Affine invariance of the reconstruction.